Bull. Nov. Comp. Center, Num. Model. in Atmosph., etc., 1 (1993), 33–67

Instability of convective cells and genesis of different scale convective structures

V.M. Malbackov and O.F. Winkenstern

The article is devoted to the theoretical investigation of atmospheric convection on the base of analytical, semi-analytical and numerical solving equations of deep and shallow convection. The studies conducted have allowed the following conclusions: the heat of convective turbulence is convective cell; convective cell is unstable to a finite-amplitude disturbances; stability of cells is determined by external model's parameters and decrease with time; complicated nature of convective turbulence is conditioned by interaction between cells resulting in their coagulation or destruction; the model accounts for only interaction of cells located over each other. This and a number of simplifications for setting up a problem make possible to construct the convective cells's distribution function depending on their sizes, existence time and large-scale parameters; there are three ierarchy levels of convective formations in atmosphere: small-scale convective turbulence, thermals and cumulus clouds, convective ensembles; rotation of convective cells causes their stability to increase by enhanced stability of rotating cells a relatively weak thermals and cumulus clouds transform to whirlwind or tornado; a tropical cyclones may be considered to be (with minor reservations) large-scale analog of whirlwind. In spite of essentially different sizes the space structure and mechanism of these phenomena has much in common, in particular, the type of circulation.

1. Simplified hydrodynamical-statistical model of interacting convective cells ensemble

1.1. Introduction

Atmospheric convection is understood to be processes connected with vertical density instable stratification of air. These processes include a wide size range of atmospheric disturbance: pulsation with size of several centimetres, thermal and cumulus clouds with size from several dozen meters up to the kilometre and also convective supercells and cloud populations covered the area from several dozen to several millions cubic kilometres. Some authors attribute to convection also a phenomena resulted from atmosphere's being thermally inhomogenious along horizontal. From this viewpoint a more wide class of processes may be reffered to as convection, including

global atmospheric circulation conditioned by a difference in solar heating upper and lower latitude and by Earth's rotation.

In this part of paper simplified approach is suggested to investigate convective turbulence. This approach is based on imagining turbulent structures as own solutions of nonlinear nonsteady thermo-hydrodynamic equations [8]. These solutions having under certain values of parameters the form of solitons in space and time shall be called the convective cells.

Simplified model suggested describes in analytic form both space-time structures of convective cells and their interaction; it takes into account the interactions being most probable in convective conditions. That is coagulation of convective cells and their destruction. The latter occures as gradient catastropha and results from convective cells being instable with respect to a finite-amplitude disturbance. The degree of cell instability depends on it's buoyancy – dimensionless parameter coinciding with precision to constant factor with inner Relei's number for this cell. The distribution function of cells depending on both their sizes and external parameters of model taking into account environment conditions was constructed. Therefore going from hydrodynamic model to statistical simulation was carried out.

Proposed hydrodynamic-statistical models show that convective turbulence with pulsation, whose amplitude not exceed a few dozen centimetres, arises on the base of molecular viscosity. Under certain conditions turbulent pulsations together with dynamic turbulence form convective cells of the following ierarchy level of sizes - thermals and cumulus clouds. And the last, in their turn, are the turbulence base for forming cloud populations of varies types. A convective formation of higher ierarchy level are not known in the Earth's atmosphere because, apparently, its being small. Convective cells of 4-th and 5-th levels can exist on the larger planets and on the sun.

Let us investigate evolution of the convective cells having two substantially different characteristic scales: pulsations of size no greater than several dozens of centimeters, generating thermal turbulence, and thermals of size about three order more, originating in this turbulent atmosphere. In this work particular attention has been given to the determination of factors causing the growth and destruction of cells, the formation of their characteristic scales, and the qualitative explanation of the turbulisation of air inside the thermals.

1.2. Mathematical formulation of the problem

Let us consider the problem about interaction of several convective cells initiating by thermal impulses setting at the initial moment. The problem

is solved under the following simplifying assumptions:

- the convection develops in the polytropic atmosphere, i.e., the temperature is linear function of height;
- vertical scales of convective cells are greater than horizontal scales and therefore, initial equations are derived from thermodynamic-equations by using simplifications of the theory of vertical boundary layer [10];
- both convective cells and thermal impulses are axisymmetric and located on the vertical axis;
- coefficient of turbulence viscosity and heat conductivity are independent on coordinates and time.

On simplifications of the convection theory and the theory of vertical boundary layer the thermohydrodynamic equations are in the form [19]:

$$\begin{aligned}
&\frac{\partial w}{\partial dt} + u\frac{\partial w}{\partial r} + w\frac{\partial w}{\partial z} = \lambda\theta + \frac{\nu}{r}\frac{\partial}{\partial r}r\frac{\partial w}{\partial r} + \nu\frac{\partial^2 w}{\partial z^2},\\
&\frac{\partial \theta}{\partial t} + u\frac{\partial \theta}{\partial r} + w\frac{\partial \theta}{\partial z} = \alpha w + \frac{\nu}{r}\frac{\partial}{\partial r}r\frac{\partial \theta}{\partial r} + \nu\frac{\partial^2 \theta}{\partial z^2},\\
&\frac{\partial ur}{\partial r} + \frac{\partial wr}{\partial z} = 0.
\end{aligned} \tag{1.1}$$

The notation used are:

t – time;

r, z – cylindrical radial and vertical coordinates;

u, w – radial and vertical components of velocity correspondingly;

ϑ – temperature deviation from it's values $\theta = \theta_0 - \gamma z$ in undisturbed atmosphere;

$\lambda = g/\theta_0$;

g – gravitational acceleration;

ν – the molecular or turbulent viscosity factor;

$\alpha = \gamma - \gamma_0$;

γ – the lapse rate of the undisturbed atmosphere,

γ_0 – the dry adiabatic lapse rate.

Prandtle number is assumed to be $Pr = 1$. There are terms allowing for influence of vertical turbulent viscosity in (1.1). Analysis shows, that these terms must be less than other terms by a factor of $\varepsilon = l(t)/h(t)^2$ (l, h – horizontal and vertical thermal's sizes being defined by the problem). Terms allowing for the influence of vertical turbulent viscosity are included at first, to investigate balance between the inertial and viscous forces and at second, because elimination of terms with the higher derivative changes the type of equations that is inadmissible here. Nevertheless solutions allowing for and not allowing for the vertical turbulence viscosity are not to be substantially different from each other, because otherwise the accepted simplifications are not valid.

Let us set initial conditions for equations (1.1). Suppose that at $t = 0$ there are no motions, and the appearance of thermals is simulated by setting at this moment of time several thermal impulses located on the vertical axis:

$$\text{at} \quad t = 0 \qquad \vartheta = \frac{4\nu^2}{\lambda r_0^2} exp\left(-\frac{r^2}{2r_0^2}\right) f_0(z), \quad w = 0, \tag{1.2}$$

where $f(z)$ is a function defining the vertical distribution ϑ, it is non-zero on several segments contacting with each other.

1.3. Solutions of the problem

Let us solve the Cauchy problem (1.1)–(1.2). The solution may be written in the form (in detail see [19])

$$\begin{aligned} w &= 4\nu^2 a(t)\varphi(t) f(z,t) exp\left(-\frac{ar^2}{2}\right), \\ u &= -\frac{4\nu^2\varphi}{r}\left(1 - exp\left(-\frac{ar^2}{2}\right)\right)\frac{\partial f}{\partial z}, \\ \vartheta &= \frac{4\nu^2 a\varphi_1(t)}{\lambda} f(z,t) exp\left(-\frac{ar^2}{2}\right), \end{aligned} \tag{1.3}$$

where

$$\varphi = \begin{cases} t & \text{at} \quad \alpha = 0, \\ \sin(\sqrt{-\alpha\lambda}t)/\sqrt{-\alpha\lambda} & \text{at} \quad \alpha < 0, \\ \sinh(\sqrt{\alpha\lambda}t)/\sqrt{\alpha\lambda} & \text{at} \quad \alpha > 0; \end{cases} \tag{1.4}$$

$$\varphi = \begin{cases} 1 & \text{at} \quad \alpha = 0, \\ \cos(\sqrt{-\alpha\lambda}t)/\sqrt{-\alpha\lambda} & \text{at} \quad \alpha < 0, \\ \cosh(\sqrt{\alpha\lambda}t)/\sqrt{\alpha\lambda} & \text{at} \quad \alpha > 0; \end{cases} \tag{1.5}$$

$$a = 1/(2\nu t + r_0^2), \tag{1.6}$$

$f(z,t)$ satisfies the equation

$$\frac{\partial f}{\partial t} + 4\nu^2 a\varphi f\frac{\partial f}{\partial z} = \nu\frac{\partial^2 f}{\partial z^2}; \tag{1.7}$$

$$\text{at} \quad t = 0 \qquad f = f_0(z). \tag{1.8}$$

At the case of neutral stratified atmosphere ($\alpha = 0$), assuming $r = 0$ and substituting v, α from (1.4), (1.6) into (1.7) we come to a problem for the linear thermal impulse randomly distributed along the axis Oz:

$$\frac{\partial f}{\partial t} + 2\nu f\frac{\partial f}{\partial z} = \nu\frac{\partial^2 f}{\partial z^2}; \tag{1.9}$$

$$\text{at} \quad t = 0 \quad f = f_0(z). \tag{1.10}$$

Equation (1.9) is the well-known Burgers equation reproduced to a linear one by substitution

$$f = F(z,t)\Big/\left(c + \int_z^\infty F dz\right)$$

as a result we have the following problem:

$$\frac{\partial F}{\partial t} = \nu\frac{\partial^2 F}{\partial z^2}; \tag{1.11}$$

$$\text{at} \quad t = 0 \quad F = cf_0 exp\int_z^\infty f_0 dz. \tag{1.12}$$

1.4. Coagulation of convective cells

In the following, let us study thermal convection caused by finite quantities of heat q instantly released at $t = 0$ in several fixed points on the axis with coordinates $z = z_i$, $(i = 1, 2, \ldots, n;\ z_{i+1} > z_i)$. The solution to the problem for this case was obtained in [19]

$$f = \frac{\sum_{i=1}^{n} b_i \exp(-\eta_i^2)}{2\sqrt{\pi\nu t}(1 + \sum_{i=1}^{n} b_i \psi(\eta_i))}, \tag{1.13}$$

where

$$\eta_i = \frac{(z - z_i)}{2\sqrt{\nu t}}, \quad \psi(\eta_i) = \frac{1}{\pi}\int_{-\eta_i}^{\infty} \exp(-\alpha^2)d\alpha,$$

$$b_1 = \exp(Q_1) - 1,$$

$$b_{j+1} = \exp(\sum_{i=1}^{j+1} Q_i) - \exp(\sum_{i=1}^{j} Q_i), \quad j = 1, \ldots, n-1,$$

$$Q_i = \frac{\lambda q_i}{8\pi c_p \rho \nu^2}, \quad \sum_{i=1}^{n} Q_i = Q_s = \frac{\lambda q_s}{8\pi c_p \rho \nu^2}, \quad Q_s = \int_{-\infty}^{\infty} f dz,$$

where Q_i, Q_s are non-dimensional constants; c_p is the heat capacity of air at constant pressure; ρ is the mean density.

The last relationship at (1.13) results from the condition of conservation of heat amount:

$$2\pi \int_0^{\infty}\int_{-\infty}^{\infty} \vartheta dz r dr = \frac{q_s}{c_p \rho}. \tag{1.14}$$

Now let us define the values of parameters such that the vertical boundary layer simplifications used could be valid. When the last term in equation (1.9) allowing for the influence of vertical turbulence is small, solution (1.13) have to be close the solution to the problem

$$\frac{\partial f}{\partial t} + 2\nu f \frac{\partial f}{\partial z} = 0, \quad \int_{-\infty}^{\infty} f dz = Q_s. \tag{1.15}$$

With $n = 2$ problem (1.15) has the following solution:

$$\text{at} \quad 0 \le t \le t_1 \quad \text{and} \quad h_1 \le z \le z_2$$

$$f = \begin{cases} (z - z_1)/2\nu t & \text{at} \quad z_1 \le z \le h_1(t), \\ (z - z_2)/2\nu t & \text{at} \quad z_2 \le z \le h_2(t), \\ 0 & \text{at} \quad z < z_1, z > h_2; \end{cases} \tag{1.16}$$

where $t_1 = (z_2 - z_1)^2/4\nu Q$, $h_1 = z_1 + 2\sqrt{Q_1 \nu t}$, $h_2 = z_2 + 2\sqrt{Q_2 \nu t}$;

$$\text{at} \quad t_1 < t \le t_2 \quad \text{and} \quad z_2 < z \le h_2$$

$$f = \begin{cases} (z - z_1)/2\nu t & \text{at} \quad z_1 \le z \le h_3(t), \\ (z - z_2)/2\nu t & \text{at} \quad z_3 \le z \le h_2(t), \\ 0 & \text{at} \quad z < z_1, z > h_2; \end{cases} \tag{1.17}$$

where $t_2 = t_1(\sqrt{Q_s} + \sqrt{Q_2})/Q_1$, $h_3 = (z_2 + z_1)/2 + 2Q_1\nu t/(z_2 - z_1)$;

$$\text{at} \quad t > t_2$$

$$f = \begin{cases} (z - z_1)/2\nu t & \text{at} \quad z_1 \leq z \leq h_4(t), \\ 0 & \text{at} \quad z < z_1, z > h_4; \end{cases} \tag{1.18}$$

where $h_4 = z_1 + 2\sqrt{Q_s\nu t}$.

Comparision of solutions allowing for and not allowing for the vertical viscosity shows its having minor influence on the process with $Q_i = \lambda q_i/(8\pi c_p \rho \nu^2) \geq 10$. Only with such parameter values vertical scales of the process prevail over the horizontal scales. For example Figure 1 gives the type of functions $f(z)$ accounting for and not accounting for vertical viscosity at different moments of time with the following parameter values:

$$n = 2, \quad Q_1 = Q_2 = 25, \quad z_1 = 0, \quad Z_2 = 600m, \quad \nu = 10m^2/s. \tag{1.19}$$

It is easily seen that at $Q_1 = Q_2 = 25$ the influence of vertical viscosity is not great – the curves 1 and 2 are close to each other. The analysis of the solution of (1.16)–(1.19) shows that the whole process can be conditionally divided into three stages begining at the moments $t = 0$, $t = t_1$ and $t = t_2$. At the first stage relationships (1.16) are valid. Thermal convection at $0 \leq t \leq t_1$ develops within two regions that are not adjoining, i.e., the thermals do not contact with each other. In all convective regions u is small and does not depend on z and w is growing with height according to the linear law, reaching it's maximum values

$$w_i = 2\sqrt{Q_i\nu/t} \quad \text{at} \quad r = 0 \quad \text{and} \quad h_i = 2\sqrt{Q_i\nu t} + z_i, \tag{1.20}$$

i.e., on the axis near the upper boundaries of the thermal, and minimum values $w = w_{min}$ at their lower boundaries $z = z_i + w_{min}t$, where $w < w_{min}$ are velocities neglibigly small for the thermals ascent. In so doing the ascent velocities of the upper boundaries appear to be lower than the maximum values of updrafts in the thermals.

Now let us consider the results of observations over the ascending thermals. We know that in real conditions the thermals expand their volume during their ascent [2], [24]. Laboratory experiments show linear variation of thermal radius with height [28]. The vertical component of motion is prevailing in the thermals; it is maximal in the upper part of the cells called thermal's core. Movements are insignificant in the lower part of the thermal called thermal's trail. The core ascent velocity appears to be less than the maximal vertical motions within the core [2]. Comparision of observational results with theoretical results shows that the obtained solution

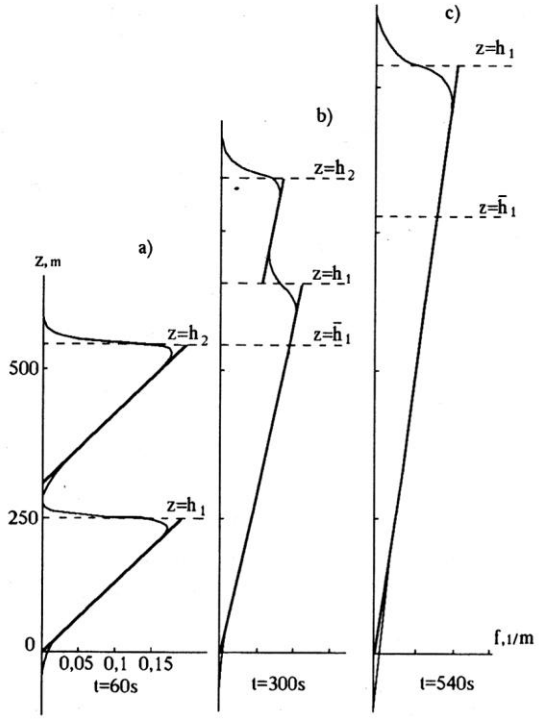

Figure 1. The type of functions $f(z)$ at different moments of time with the following parameter values: $n = 2$, $Q_1 = Q_2 = 25$, $z_1 = 0$, $Z_2 = 600m$, $\nu = 10m^2/s$. Thin line – the solution accounting for vertical viscosity, bold line – the solution not accounting for vertical viscosity; $z = h_1$ and $z = h_2$ – maximal vertical size of thermals; $z = \bar{h_1}$ – maximal vertical size of the lower thermal in the case that the upper thermal is absent.

qualitively describes the major features of distribution of meteorological element's fields in the thermals.

Let us consider the mechanism of interaction of the thermals. The stage of interaction begins at $t = t_1$. At this moment the upper boundary of the lower thermal reaches the level $z = z_2$ the velocity of it's movement increases. So the velocity of movement of an isolated thermal decays in time: $dh_1/dt = \sqrt{Q_1\nu/t}$, while during interaction this velocity is already constant and equals $dh_1/dt = 2\nu Q_1(z_2 - z_1)$. So the ascent velocity of the lower thermal increases due to it's interaction with the upper thermal. To the same conclusion one comes experimentally [28]. As the velocity of the upper boundary of the upper thermal also decays $v_2 = dh_2/dt = \sqrt{Q_2\nu/t}$, the lower thermal completely absorbs the upper one with time. This takes place at $t = t_2$. The new thermal formed at this moment

does not differ from the thermal formed under the influence of one impulse with power $q_s = q_1 + q_2$, given at $t = 0$, $r = 0$, $z = z_1$. Note that the effect of coagulation of the thermals is conditioned by the influence of nonlinear dynamic factors: any linearization of equations is inadmissible, because then no coagulation of thermals will happen due to the principle of suprposition. So, for example, in this case the lower more powerfull thermal can go through the upper one, and then two thermals will again exist independently.

Therefore the dynamic entrainment is the important factor bringing to the growth of convective cells. Ludlam and Scorer [15] came to the same conclusion; according to their investigations the total mass of the captured thermals can substantially exceed the mass of the mother cell. As a result the latter rises much higher. It will be shown below that the interaction can lead not only to the growth of thermuls but also to their destruction.

Unfortunately the observational data concerning the interaction of atmospheric thermals are not known to us. The work [28] describes the laboratory finding concerning simulation of this processes in laboratory set up: portions of fluid lighter in weight than water (water solution of special chemical) were introduced into water in equal time intervals. As a result thermals were obtained having similar buoancy and similar path of ascent. So it arises the system consisting of three interacting thermals located over each other. Experiments have shown that the upper boundary of the first thermal rose at the rate $v \sim 1/\sqrt{t}$. The second thermal moved upward at larger rate but the upper boundary of the third lowest thermal moved already at the rate equal to that of the second thermal.

Let us compare experimental conclusions with theoretical results. For this purpose we take the solution to the problem describing the interaction of three similar ($Q_1 = Q_2 = Q_3 = Q/3$) thermals located on equal distance ($z_2 - z_1 = z_3 - z_2$) without vertical turbulence:

$$f = \begin{cases} (z - z_1)/2\nu t & \text{at} \quad z_1 \le z \le h_1, \\ (z - z_2)/2\nu t & \text{at} \quad h_1 \le z \le h_2, \\ (z - z_3)/2\nu t & \text{at} \quad h_2 \le z \le h_3, \\ 0 & \text{at} \quad z < z_1, \quad z > z_3, \end{cases}$$

where

$$h_1 = \frac{2Q_1\nu t}{z_2 - z_1} + \frac{z_2 - z_1}{2}, \quad h_2 = \frac{2Q_1\nu t}{z_3 - z_2} + \frac{z_3 + z_2}{2},$$

$$h_3 = 2\sqrt{Q_3\nu t} + z_3, \quad t_1 = \frac{(z_2 - z_1)^2}{4\nu Q_1}, \quad t_2 = t_1(3 + 2\sqrt{2}).$$

This solution is in the time interval $t_1 < t < t_2$, where t_1 corresponds to the moment of time when the lower thermal "catches up with" the middle one. At the same moment the core of the middle thermal appeares to be in the trace of the upper thermal. The value t_2 corresponds to the moment of time when the upper thermal coalesces with the middle termal.

Now let us define rise velocifies of upper boundaries of the thermals. It is easely seen that the vertical movement velocity of the upper thermal decays: $v_3 = dh_3/dt \sim 1/\sqrt{t}$, and that the middle thermal rises quicker than the upper one: $v_3 = dh_2/dt = 2\nu Q_2/(z_3 - z_2)$, but the velocities of the lower thermal and middle thermal upper boundaries are the same: $v_1 = v_2$. So this model describes regularities established experimentally.

Let us investigate thermal evolution in a stably ($\alpha < 0$) and instably ($\alpha > 0$) stratified atmosphere. The similarity of solutions to the problems (1.7), (1.8) and to the problem without turbulent viscosity will show the range of values of external parameters such that our theory could be applied

$$\frac{\partial f}{\partial t} + 4\nu^2 a\varphi f \frac{\partial f}{\partial z} = 0, \quad \text{at} \quad t = 0 \quad f = f_0(z). \tag{1.21}$$

Solutions (1.21) at $\alpha < 0$ and at $\alpha > 0$ for one thermal impulse are obtained in the work [19]. Solution in the stable atmosphere (as well as at $\alpha = 0$) appeared to be valid only when thermal impulses are sufficiently strong, but in contrast to neutral stratification the thermal core reaches maximal heights long before the complete decay of convection. Once the growth in the vertical has stoped, horizontal sizes of a thermal gradually approach vertical sizes. For this reason the applicability of the theory for $\alpha < 0$ is limited also in time. At $\alpha > 0$ the power of initial thermal impulse is not substantial because thermal convection is maintained by the energy of instability, and the simplifications of vertical boundary layer appear to be valid due to the substantially more rapid increase of vertical scales of the phenomenon in comparision with the horizontal scales.

It is not difficult to obtain the solutions to (1.21) at $\alpha > 0$ and $\alpha < 0$ and for the case of two thermal impulses. The analysis of these solutions (we do not give them because of their awkwardness) shows that the character of interaction of thermals is about the same as at $\alpha = 0$. The difference with the case $\alpha = 0$ is in the interaction's taking place either quicker (at $\alpha > 0$) or slower (at $\alpha < 0$) due to more rapid or slow increase of the vertical sizes of the thermals.

1.5. Instability of convective cells

Let us show that relations (1.13) lose their physical meaning at certain critical parameter values due to the violation of balance between the inertial

and viscous forces. Let us define critical parameter values and investigate the behaviour of the function f at the parameter values that are close to critical values. In considering the case of atmospheric exposure to two thermal impulses, we suggest that the first impulse is caused by a powerfull thermal influence with $Q_1 > 10$, and the second very weak thermal influence with $Q_2 = \varepsilon \ll 1$ is caused by occasional fluctuations in the temperature field. In this case

$$b_1 = \exp(Q_1) - 1 \approx \exp(Q_1), \quad b_2 = \exp(Q_1 + \varepsilon) - \exp(Q_1) \approx \exp(Q_1).$$

After substitution b_1 and b_2 into (1.13) we have:

$$f = \frac{\exp(Q_1)\exp(-\eta_1^2) + \varepsilon \exp(-\eta_2^2)}{2\sqrt{\pi\nu t}(1 + \exp(Q_1)(\psi(\eta_1) + \varepsilon\psi(\eta_2)))}. \tag{1.22}$$

The denominator in (1.22) vanishes and the solution makes no sense at

$$\varepsilon = -\frac{\exp(Q_1) + \psi(\eta_1)}{\psi(\eta_2)}. \tag{1.23}$$

So the values ε depend on t, t_1, z, z_1, z_2, but as fluctuations in the temperature field can appear at any moment of time and at any point of space, then minimal modulus value of ε should be taken from (1.23). This value corresponds to the minimal in "power" thermal fluctuation, destroying the thermal; it is reached at $\psi(\eta_1) = \psi(\infty) = 0$ and $\psi(\eta_2) = \psi(-\infty) = 1$. Substituting these values into (1.23), we finally have:

$$\varepsilon = \varepsilon_{cr} = -\exp(-Q_1). \tag{1.24}$$

Weaker fluctuations do not destroy the thermal. It is easily seen that $f \to 0$ at $\eta_1 \to \infty$, $\eta_2 \to -\infty$. But at $\varepsilon \to \varepsilon_{cr}$ depending on z_1 and z_2 the numerator in (1.22) vanishes quicker than the denominator in certain space points. Calculation showed that at $\varepsilon \to \varepsilon_{cr}$ accidental perturbations over the upper boundary are most "dangerous" for the convective cell. Abrupt increase of temperature, velocity and lapse rate takes place in the thermal core, and a region with downdraughts and negative temperature deviations, resembling a turned over convective cell, appears over the core. The solution behaviour at this case resembles the stage preceding the wave turnover . But the turnover itself cannot take place in the theory considered here because it is prohibited by the form of the solution (1.3) itself (f – values cannot have different signs at fixed heights). That is why the so-called gradient catasrophe took place in the calculations at the ε – values that are very close to the critical value: the solution had a discontinuity at

a transition from $f \to \infty$ to $f \to -\infty$ in it's passage through the point of dicontinuity. This means absolute disagreement between the inertial and viscous forces and the beginning of the formation of turbulent pulsations, the process that cannot be discribed by the given simplified model.

The established regularities take place in nature during convective process on different scales. So a turned over cell, located over a powerfull cumulus cloud is a common atmospheric phenomenon [2], [17].

Let us briefly describe another natural phenomenon that can be partly explained with the help of our theory. Convective boundary layer forming during the day in summer over vast territories is always limited from above by a thin inversion layer that is called entrainment region. It is known that the entrainment region is the product of interaction of convective cells with the air above them. Mixing of two air masses taking place in this region can be explained by the inertial instability of movements in the thermals, that constitute a convective ensemble. The process of mixing, as shown by this model, can be related to the effects of the "wave turnover" [6], [27] and associated entrainment into the movement of air masses above the thermals.

The effects of wave turnover are also well-known at microscale convection. For example, the length of laminar thermal flow over a smouldering cigarette is 10–20 cm. Above that the flow decomposes into separate eddy formations of a lesser size.

Let us define maximal sizes of convective cells. Consider for this purpose the relation (1.24): it shows that the stronger the initial influence on the atmosphere, the weaker the hydrodynamic stability of the convective formation it caused. In the case when the convective cell is formed by coalescence of several thermals it's stability is the weaker, the more heat in the region covered by convection.

If we accept air viscocity as molecular: $\nu \approx 2 \cdot 10^{-5} m^2 s^{-1}$ and $\lambda = 0,33 m\ s^{-2}\ {}^0K$, $\rho = 10^3 g\ m^{-3}$, $Q_1 = 25$, then, as can be easily calculated by (1.13), (1.24), thermal perturbation equal to $q_2 = -4 \cdot 10^{-10} cal$, is sufficient for the microscale convective cell to lose it's stability. Random perturbations on such scale can be realized even at the expense of the thermal movement of molecules.

If the medium is considered to be turbulent, then at $\nu = 10 m^2\ s$ and $Q_1 = 25$ turbulent pulsations in the temperature field of power $q_2 = -1 cal$ lead to the "destruction" of a convective cell. Naturally such a cell is very close to instability. When Q_1 becomes greater instability catstrophically increases. For example, at $Q_1 = 100$ effects, 30 orders of magnitude smaller than at $Q_1 = 25$ cause the "destruction" of a cell.

Using the obtained solutions, it can be easily shown that the vertical

sizes h are related to the horizontal l sizes of thermals as

$$n = h/l = \sqrt{Q_1}. \tag{1.25}$$

The relationships (1.25) shows that the more difference of the vertical and the horizontal scales of a convective cell, the weaker the inertial stability of this formation. Indeed, observations show that convective cells with approximately the same vertical and horizontal sizes are encountered more often [2].

Thus the proposed theory is applicable in the following range of Q_s – values:

$$10 \leq Q_s \leq Q_c \approx 25. \tag{1.26}$$

At $Q_s < 10$ h and l differ insignificantly and hence vertical boundary layer simplifications we used during the derivation of initial equations are not applicable; at $Q_s > Q_c$ the cell is unstable.

Let us define maximal scales of convective turbulent pulsations and maximal scales of the thermals using (1.26). Assuming $i = 1$, $Q_1 = Q_c$, $z_1 = 0$ in (1.20) we have:

$$t_c = 4Q_c\nu/w_m^2, \quad h_c = 2\sqrt{Q_c\nu t_c}, \tag{1.27}$$

where t_c is the time of development of a convective cell; w_m is the minimal vertical velocity component in a cell for the convective formations of this type; h_c is the characteristic vertical scale of a cell.

Assuming molecular air viscosity $\nu = 2 \cdot 10^{-5} m^2/s$, at $Q = 25$, $w = 10^{-2} m/s$, we have $t = 20s$, $h = 20sm$ – the continuous region of thermal flow over the smoudering cigarette has just the same length. The turbulent medium, where the thermals originate, is formed by thermally induced pulsations along with turbulent perturbations caused by the shear instability of the external flow.

Assuming the medium to be a turbulent one, at $\nu = 10\ m^2/s$ and $w = 1\ m/s$, we have the following maximal values of spatial-time scales for the thermals: $h_c = 10^3 m$, $t = 10^3 s$. The observations confirm the obtained value.

We note, however, that in real conditions the cell reaches the maximal sizes, apparently, at the stage of maximal evolution, while according to (1.27) it occures at the stage of process dissipation. It can be simply explained: real thermals develop, as a rule, spontaneously, owing to instability energy. But the relations (1.27) do not take into account the influence of stratification on the process. Let us assess this influence on the evolution of convective cells. Characteristic time scales of gravitational

waves (at $a < 0$) and time of their existence (at $a > 0$) are known to be determined by the Brunt-Vaisala frequency:

$$t_b = 2\pi/\sqrt{|\alpha|\lambda}. \tag{1.28}$$

Substituting into (1.28) $\alpha = 3 \cdot 10^{-3}\ {}^0K/m$ and $\alpha = -3 \cdot 10^{-3}\ {}^0K/m$, corresponding to the unstable and stable stratifications of air, at $\lambda = 0,033\ m/(s^2\ {}^0K)^{-1}$ we have $t_b = 600\ s$. In the case of molecular air viscosity $t_c \ll t_b$. So the stratification of air must not influence on the scales of convective pulsations generating atmospheric turbulence. Thin surface layer where the value α can be 2–3 orders of magnitude larger than its characteristic values, makes an exception. This property is taken into account in the parameterization models of the constant flows' atmospheric layer [6].

In the case of turbulent atmosphere $t_c > t_b$ and hence the stratification of air must already play a substantial role in the formation of thermals.

1.6. Convection under the unstable stratification of atmosphere

Assuming that $\alpha > 0$, $r_0 = 0$ in (1.4)–(1.6) and substituting their values into (1.7) we have

$$\frac{\partial f}{\partial t} + \frac{2\nu \sinh(\sqrt{\alpha\lambda}\, t)}{\sqrt{\alpha\lambda}\, t} f \frac{\partial f}{\partial z} = \nu \frac{\partial^2 f}{\partial z^2}. \tag{1.29}$$

Function f must satisfy the following integral condition:

$$\int_{-\infty}^{\infty} f\, dz = Q_\varepsilon, \quad Q_\varepsilon = \frac{\lambda q_\varepsilon}{8\pi c_p \rho \nu^2}, \tag{1.30}$$

where q_ε is the amount of heat released at the moment $t = 0$. The total amount of heat in the region covered by convection increases with time

$$\frac{q_s}{c_p\rho} = 2\pi \int_0^{\infty} \int_{-\infty}^{0} \vartheta\, dzrdr = \frac{\cosh(\sqrt{\alpha\lambda}\, t)}{c_p\rho}. \tag{1.31}$$

Problem (1.29), (1.30) was solved numerically. Several numerical schemes were used and all of them were no longer stable at $t > t_c$. The time of beginning instability and "the form" of it's realization depended on the scheme chosen. However this dependence was weak with time-space steps

being sufficiently small; in this case instability took place at value Q_s ranged from 25 to 100:

$$Q_s = Q_c = Q_\varepsilon \cosh(\sqrt{\alpha\lambda}\, t) \approx 25 \div 100. \tag{1.32}$$

Comparision of (1.26) and (1.32) allows to conclude that whatever the stratification of atmosphere the convective cell remains stable only when the heat amount contained by one does not exceed some critical value defined by the relations (1.26), (1.32).

The numerical solution of problem (1.29), (1.30) corresponds sufficiently well to the analitical solution of problem (1.21) obtained in [19], corresponding to $\alpha > 0$ for the case when vertical viscosity is neglected. The approximate form of this solution carried out at $t \gg 1/\sqrt{\alpha\lambda}$:

$$\begin{aligned}
&\text{at} \quad 0 \le z \le h, \quad h = 2\sqrt{\frac{Q_\varepsilon \nu \exp(\sqrt{\alpha\lambda}\, t)}{\sqrt{\alpha\lambda}}} \\
&w = \sqrt{\alpha\lambda}\, z \exp(-\eta^2) \\
&u = -\frac{2\nu\sqrt{\alpha\lambda}}{r}(1 - \exp(-\eta^2)) \\
&\vartheta = \alpha z \exp(-\eta^2) \\
&\text{at} \quad z < 0 \text{ and } z > 0 \quad w = u = \vartheta = 0.
\end{aligned} \tag{1.33}$$

The expressions for the critical velocity value w_c. The convective cell maximal height h_c and the time of cell existence t_c, obtained with the help of (1.32), (1.33) have the following form:

$$t_c = \frac{1}{\sqrt{\alpha\lambda}} \ln\left(\frac{Q_c}{Q_\varepsilon}\right), \quad h_c = 2\sqrt{\frac{Q_c\nu}{\sqrt{\alpha\lambda}}}, \quad w_c = 2\sqrt{Q_c\nu\sqrt{\alpha\lambda}}. \tag{1.34}$$

Assuming $\alpha = 3 \cdot 10^{-3}\ {}^0K\ m$, $\lambda = 0{,}033 m/(s^2\ {}^0K)$, $\nu = 10 m^2/s$, $Q_c = 25$ and substituting these values into (1.34) we obtain $h_c = 640m$, $w_c = 3{,}2 m/s$, that is close to value observed in the real thermals.

It should be noted that air movements within the atmospheric boundary layer are very diverse and spontaneous. The theory developed here does not describe all the diversity of forms of atmospheric convective cells, but it qualitively explains the reason of this diversity. It is in that all sufficiently developed cells are unstable relative to finite amplitude perturbations. The theory does not give a definite answer to the question of how does the realization of instability occure, but, obviously, the form of resolution instability is different for the cells of different intensity. The

reason of beginning of cells destruction is also different. "Powerful" cells are unstable to very weak perturbations caused by random fluctuations in the temperature field. Weaker thermals can be destructed as a result of their interaction with the cells in the downdraughts and the air that is colder than the environment. There can be many other reasons of instability of movements in the thermals that are not considered by this simplified model; for example, the processes of interactions of cells with each other and with the environment, taking place on the sides of the thermals (due to the simplifications of the vertical boundary layer theory, made in derivation of initial equations, the conclusions of the theory lose their phisical meaning at a long distance from the axis of thermals). None the less the mentioned processes: dissipation, spontaneous growth, interaction of thermals cause the diversity of the forms of movements that take place in the convective boundary layer; nonlinear interaction causes both the growth and the destruction of thermals.

1.7. Statistical characteristics of an ensemble of thermals

Let us consider the unstable atmosphere again. At $\alpha > 0$ the buoyancy of thermals increases with time due to instability energy. As the buoyancy increases from Q to $Q + dQ$ the probability of cell's destruction is defined according to (1.24) as

$$S(Q)\, dQ = \exp(-Q)\, dQ, \tag{1.35}$$

the following being fulfilled

$$\int_0^\infty \exp(-Q)\, dQ = 1. \tag{1.36}$$

If the theory is correct at $Q \geq Q_\varepsilon$, then we have in place of (1.35), (1.36)

$$S(Q)\, dQ = \exp(Q_\varepsilon - Q)\, dQ, \quad \int_{Q_\varepsilon}^\infty \exp(Q_\varepsilon - Q)\, dQ = 1. \tag{1.37}$$

The relationships (1.35) is convenient for calculations to be written at the term of vertical thermals's sizes $S(h)$ or of their existence times of $S(t)$ or of oscillation frequency $S(n)$, where $n = 1/t$. For this purpose we use (1.31), (1.33)

$$Q_s = Q_\varepsilon \cosh(\sqrt{\alpha\lambda}) \approx Q_\varepsilon \exp(\sqrt{\alpha\lambda}), \quad h = 2\sqrt{\frac{Q_s}{\sqrt{\alpha\lambda}}}. \tag{1.38}$$

Using the dependence between Q_s and h, Q_s and t, Q_s and n we have in place of (1.35)

$$S(h)\,dh = \frac{h}{h_0^2}\exp\left(-\frac{h^2}{2h_0^2}\right)dh, \quad h_0 = \sqrt{\frac{2\nu}{\sqrt{\alpha\lambda}}}; \tag{1.39}$$

$$S(t)\,dt = Q_\varepsilon\sqrt{\alpha\lambda}\,\exp(\sqrt{\alpha\lambda} - Q_\varepsilon\,\exp(\sqrt{\alpha\lambda}\,t))\,dt; \tag{1.40}$$

$$S(n)\,dn = -\frac{Q_\varepsilon\sqrt{\alpha\lambda}}{n^2}\exp\left(\frac{\sqrt{\alpha\lambda}}{n} - Q_\varepsilon\,\exp\left(\frac{\sqrt{\alpha\lambda}}{n}\right)\right)dn. \tag{1.41}$$

Obviously, expression (1.39) is most convenient, because in this case the spectral size distribution density of thermals

$$hS(h) = \left(\frac{h}{h_0}\right)^2\exp\left(-\frac{h^2}{2h_0^2}\right), \tag{1.42}$$

is the second moment of normal distribution. Let us show that other values characterizing an ensemble can be expressed through the moments of normal distribution. Let $\triangle S$ be an area of a cell of large scale model grid. Let this cell contain N thermals, whose interaction being neglected. At first we are to determine $S_{\bar{\vartheta}}(h)$, where $\bar{\vartheta}$ is excess of temperature in the cell due to collective action of thermals. The area of thermal's horizontal section is assumed to be much smaller than $\triangle S$: $\pi r_0^2 \ll \triangle S$, where $r_0 = \sqrt{5/a}$. All of the thermals are assumed to arise simultaneously at $t = 0$. At $t > 0$ they grow spontaneously and are destructed, until at $t = \triangle t$, where $\triangle t$ being time step of large-scale model, the convection reaches "satiation", i.e., $\triangle S = \pi r_0^2 N$. Therefore the model is ready for the parameterization purpose. Then all cycle is repeated already with the large-scale parameters changed for the time $\triangle t$. Using ϑ from (1.33), $S(h)$ from (1.39) and averaging in $\triangle S$ we have:

$$S_{\bar{\vartheta}}(h) = \frac{2\pi N\alpha}{\triangle S}hS(h)\int_0^\infty \exp(-ar^2)\,rdr = \frac{\alpha\sqrt{\pi}h^2}{10h_0^2}\exp\left(-\frac{h^2}{2h_0^2}\right). \tag{1.43}$$

It also can be shown that

$$S_{\bar{w}}(h) \sim h^2\exp\left(-\frac{h^2}{2h_0^2}\right), \tag{1.44}$$

$$S_{\overline{w\vartheta}}(h) \sim h^3\exp\left(-\frac{h^2}{2h_0^2}\right). \tag{1.45}$$

1.8. Comparision of calculated results with observation data

Comparision of calculated results with observation data is illustrated in Figures 2–5. In Figure 2 two curves are given: bold – convective cells size distribution calculated with the use (1.39) at $\alpha = 3 \cdot 10^{-3}\ ^0K/m$, $\lambda = 0.033m/(s^2\ ^0K)$, $\nu = 5m^2/s$; thin – distribution constructed with the use of measuring by Wolfson [15]. Figure 3 demonstrates the values $\frac{nS_{w\vartheta}}{\sigma_\vartheta \sigma_w}$ (σ_ϑ, σ_w – standard deviations ϑ and w) measured in [3] and one calculated at $\alpha = 10^{-3}\ ^0K/m$, $\lambda = 0.033m/(s^2\ ^0K)$, $Q_\varepsilon = 0,1$, $h_0 = 265m$. Figure 4 shows the average (over the lower 300-meter layer) values $nS_\vartheta(n)\sigma_\vartheta$, $nS_w(n)\sigma_w$ measured at [3] and one calculated at $\alpha = 5 \cdot 10^{-4}\ ^0K/m$, $\lambda = 0.033m/(s^2\ ^0K)$, $Q_\varepsilon = 0,1$ (note that S_ϑ and S_w coincide at the model). Figure 5 corresponds to Figure 4 only with measuring being carried out at other day and calculations being carried out at $\alpha = 10^{-3}\ ^0K/m$.

It is seen in Figures 2–5 that the model gives more "compact" distribution as compared with measuring. This fact can be partially explained by defects of the theory. But main reason, apparently, is low-frequency part of the spectrum corresponding to a formations greater than thermals being not filtered. So the second weaker maxima located at low-frequency part of the spectrum in Figures 4, 5 are pointed out at [3] to correspond to the clouds *Cu hum*. The cloudness of 3-4 ball takes place in both cases. Although lower boundary of the clouds is located at a height near 1 kilometre, it's influence was observed near the surface.

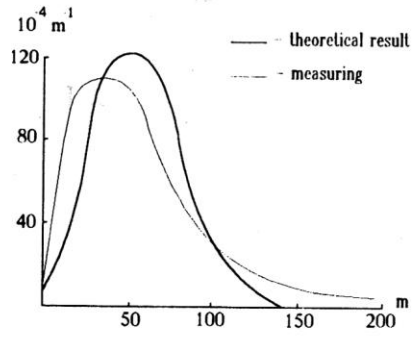

Figure 2. Comparision of calculated results with observation data: convective cells size distribution

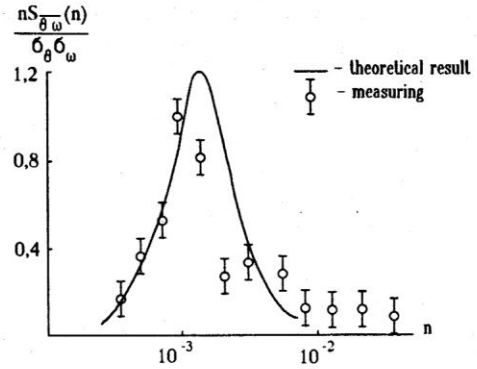

Figure 3. Comparision of calculated results with observation data: averaged normalized spectral density of vertical convective flux of heat at $z = 265m$

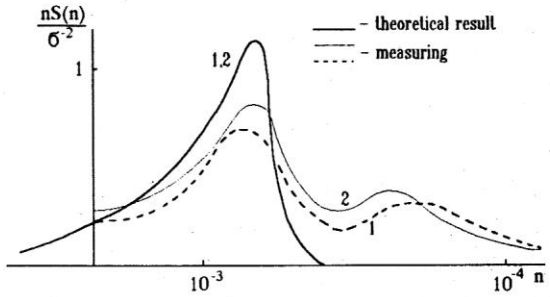

Figure 4. Comparision of calculated results with observation data: averaged spectrum of temperature (1) and velocity (2) in 300 m thick layer (7 July 1970)

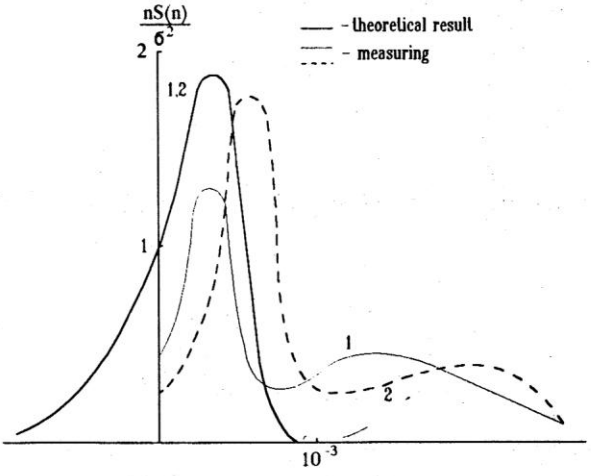

Figure 5. Comparision of calculated results with observation data: averaged spectrum of temperature (1) and velocity (2) in 300 m thick layer (7 August 1971)

1.9. Comparision results obtained by analytic model, numerical vortex-permiting model and observation data

Comparative analysis of maximal vertical velocities and maximal horizontal thermals's sizes obtained by measuring data [27] and numerical results by model of dry thermals's ensemble is given in [4]. Using (1.39), (1.40) the following correlation can be obtained

$$S(w_{max}) = \frac{w_{max}}{w_0^2}\ exp(-\frac{w_{max}}{w_0^2}), \quad w_{max} = \sqrt{\alpha\lambda}\ h, \quad w_0 = \sqrt{2\sqrt{\alpha\lambda}},$$

$$S(l) = \frac{Q_\varepsilon l}{h_0^2}\ \exp\left(\frac{l^2}{2h_0^2} - Q_\varepsilon \exp\left(\frac{l^2}{2h_0^2}\right)\right), \quad l = 2\sqrt{\nu t}.$$

Figures 6, 7 illustrate numerical and analytical results and measuring data obtained by Konovalov [12], who distinguishes two types of thermals: a) with main and a few second maxima; b) with the only maximum. In Figures 6, 7 solid cycle-points correspond to thermals of type a), cross-point – to thermals of type b), hollow cycle-point – to numerical results, solid lines – analytical results at $w_0 = 1,5m/s$, $h_0 = 150m$, $Q_\varepsilon = 0,001$. The coincidence of the results of both models and one measuring is satisfactory. Analytic model gives more compact horizontal size distribution of thermals. It may be explained by the real thermals's consisting of a few close located cells, but in the analytic model the thermals have to be widely spaced because the lateral interaction's being neglected.

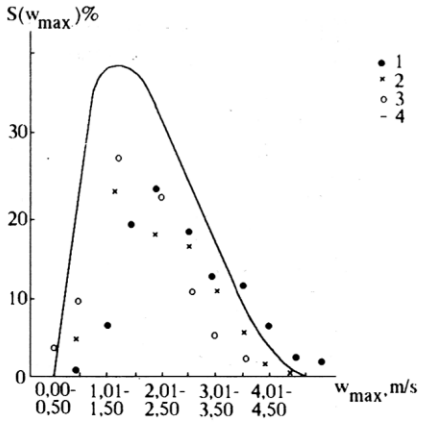

Figure 6. Comparision of calculated results with observation data: repeatability of maximal vertical velocity in thermals; (1) – thermals of type a), (2) – thermals of type b), (3) – numerical model, (4) – analytical model

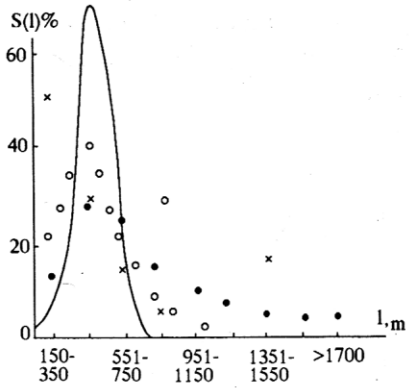

Figure 7. Comparision of calculated results with observation data: repeatability of maximal horizontal size of thermals; symbols are used as in Figure 6

1.10. Comparision of the theory with observation data concerned the distribution of convective clouds and convective ensemble

In the work [15] the theory analogous to one suggested in this paper was extended to the case of moist convection. In the same place it was shown that the expressions (1.39) may be used for the size distribution of clouds and that formula (1.39) describes satisfactorily the real distributions of convective clouds.

Let us try to use the statistical model to determine the spectrum of cloudy ensemble. The relations (1.39)–(1.41) should be changed, because the hypotheses used before about equality of horizontal and vertical viscosity is unsuitable: the main elements of horizontal turbulent transfer being in cloud populations are thermals and clouds. Let μ be horizontal turbulence coefficient, ν describe as early the vertical turbulence, μ can be greater by some order of magnitude ν in dependence on the type of cloud populations. Hence we have the following expression for l : $l_k = l/\varepsilon$, $\varepsilon = \sqrt{\mu/\nu}$. Substituting the new value $Q_k = \varepsilon h^2/l_k$ instead of $Q_H = h^2/l^2$ we obtain the horizontal size distribution of cloud population

$$S(l_k)\, dl_k = \frac{2\varepsilon h^2}{l_k} \exp\left(-\frac{\varepsilon h^2}{l_k^2}\right) dl_k. \tag{1.46}$$

Let us compare the theory with observation data. Sufficiently reliable data are included in the reference book [5]. Figure 8 shows distribution density of distance between cloud bank l_k in the Cb-type field observed (cycle) and calculated by (1.46) $S(l_k)$ (solid line). Calculations was carried out at $h = 5km$, $\varepsilon = 1/24$. Figure 9 shows distribution density of Ci–and

Cs–type cloudness measured (hollow cycle-point) and calculated by (1.39) $h = 1km$, $\varepsilon = 1/187500$ (bold line). So statistical model can be seen to give the realistic results.

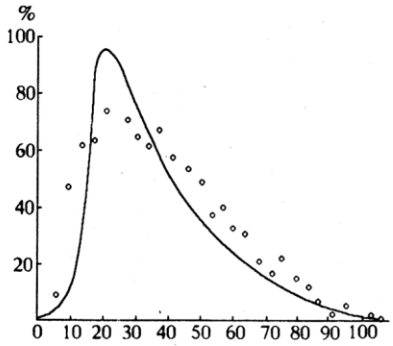

Figure 8. Distribution density of distance between cloud bank l_k in the Cb – type field observed (cycle) and calculated by (1.46) $S(l_k)$ (solid line)

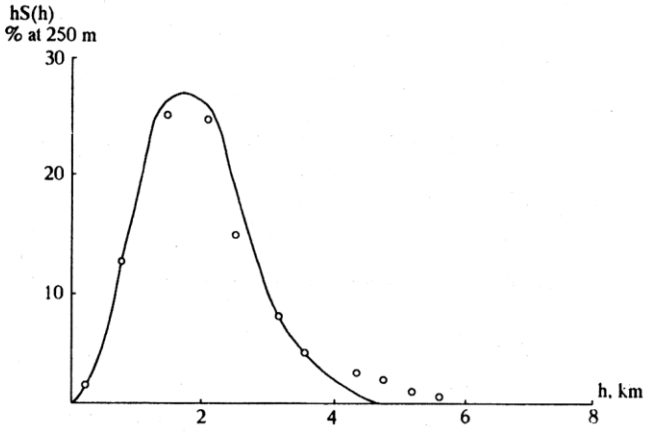

Figure 9. Distribution density of Ci – and Cs – type cloudness measured (hollow cycle-points) and calculated by (1.39) $h = 1km$, $\varepsilon = 1/187500$ (bold line)

2. Stabilizing influence of convective cells rotation on convection

2.1. Introduction

Enhanced stability of rotating systems is generally known. The example is hyroscope and geostrophic large-scale atmospheric and oceanic motions on

rotating Earth. Another example is stabilizing influence of rotation on the water outflow from the bath through the little opening in the bottom.

The analytic solutions received in this paper show that in the presence of rotative moment in the atmosphere relatively weak thermal and convective clouds can be transformed in whirlwind or tornado.

Moreover, in this paper an attempt was made to ground the hypotheses about tropic cyclone's being large-scale analog of whirlwind. The proposed numerical model demonstrates the / weak cyclonic disturbance's resulting in taiphun of middle intensity by cloudy convection, the source of angular moment being Coriolis's forces.

2.2. Time-space structure of whirlwind

In the atmosphere mesoscale vortices with vertical axis form sufficiently often. These vortices are reffered to as whirlwind, tornado. Their diameter range is from a few meteres to something like one kilometre. However this phenomena have general features, they are as follows

- vertical size is greater than horizontal;
- stratification of the atmosphere layer giving rise to vortices is dry or moist unstable;
- the sense of rotation may be different.

Last two properties point out, firstly, the energy's of instability playing essentially role and, secondly, Coriolis's force's slight influencing on the processes. That allows to assume that the mechanism of this vorticies is the same and the difference is in general quantitative. Thus the theory described this phenomena can be received on the base of general theory of mesoscale vorticies with vertical axis. The review concerned the development of this theory is given in [10]. The numerical model proposed in [12] shows the whirlwind's being the convective cell with essentially changed time-space structure. The changes are influenced by the rotation of the air particles about the cell axis.

Let us dwell on the discription of time-space vortex structure received in [12]. The calculations carried out allow to ascertain several stages in the vortex life cycle. On the first stage the convective cell is formed. The second stage begins after instaneous rotative impulse's setting on the side boundaries of calculation region. At this stage rotative impuls is moved towards axis by radial transfer. Thus the rotative component increases within vortex core and decreases at vortex periphery. At the stage of development meteorological fields within the convective cell vary insignificantly although

rotative velocity component v reaches the value $25m/s$. The third stage begins when maximal value v reaches value typical for mature tornado. During the third stage the part of kinetic energy of vortex motion come back to the system of vertical circulation and rebuilding of convective cell meteorological fields occure. At the beginning of stage short narrow current looking like funnel forms in the upper part of vortex. Descending current intensifies gradually and spreads downward. In some case the funnel nearly reaches the surface. The mature vortex stage is followed by the stage of dissipation. It should be noted, however, that the accuracy of calculation was small at the last stage. Moreover the numerical model is complicated enough to interpret the results obtained with it's help. The simplified analytic models will be proposed below:
linear – to explaine the time variations of convective cell structure ;
nonlinear – to explaine the variations of the space structure of convective cell at mature vortex stage.

2.3. Simplified linear analytical model of the vortex life cycle

In the vortex evolution area the convective cell is assumed to create the layer in which air is moving towards cell axis and rising according to continuity equation:

$$u = -\frac{br}{2}, \quad w = bz. \tag{2.1}$$

Inverse influence of vortex rotation on motion in the vertical section is ignored. In this case (2.1) is given as:

$$\frac{\partial v}{\partial t} - \frac{br}{2}\frac{\partial v}{\partial r} + bz\frac{\partial v}{\partial z} - \frac{bru}{2} = \nu\frac{\partial}{\partial r}\frac{1}{r}\frac{\partial vr}{\partial r} + \mu\frac{\partial^2 v}{\partial z^2}. \tag{2.2}$$

It is convinient to introduce rotative moment Γ in place of v

$$\Gamma = vr, \quad \frac{\partial \Gamma}{\partial t} - \frac{br}{2}\frac{\partial \Gamma}{\partial r} + bz\frac{\partial \Gamma}{\partial z} = \nu r\frac{\partial}{\partial r}\frac{1}{r}\frac{\partial \Gamma}{\partial r} + \mu\frac{\partial^2 \Gamma}{\partial z^2}. \tag{2.3}$$

Assume that Γ is independent on z and introduce new radial coordinate y:

$$\Gamma = \Gamma(y,t), \quad y = r^2/2. \tag{2.4}$$

Then it is in place of (2.3)

$$\frac{\partial \Gamma}{\partial t} - by\frac{\partial \Gamma}{\partial y} = 2\nu y\frac{\partial^2 \Gamma}{\partial y^2}. \tag{2.5}$$

The solution of equation (2.5) is to satisfy the boundary conditions:

$$\Gamma = 0 \quad \text{at} \quad y = 0 \quad \text{and at} \quad y = \infty. \tag{2.6}$$

The solution of problem (2.5), (2.6) is found in the form:

$$\Gamma = A(t) y \exp(-ay). \tag{2.7}$$

Functions $A(t)$ and a satisfy the equation

$$A' = (b - 4na)A, \quad a' = ba - 2\nu a^2. \tag{2.8}$$

and may be written as:

$$a = \frac{b\exp(bt)}{2\nu(\exp(bt)+c)}, \quad A = \frac{A_0\exp(bt)}{2\nu(\exp(bt)+c)^2}, \quad v = \frac{Ar}{2}\exp\left(-\frac{ar}{2}\right). \tag{2.9}$$

To find the constant c and A_0 we demand

$$\text{at} \quad t = 0, \quad v_m = v_1, \quad r_m = r_1, \tag{2.10}$$

where $r = r_m$ is value of r, at which v reaches a maximum $v = v_m$. Let at (2.9) $\frac{\partial v}{\partial r} = 0$, then

$$r_m = \frac{1}{\sqrt{a}}, \quad v_m = \frac{A\exp(-0,5)}{2\sqrt{a}} \tag{2.11}$$

and at $t = 0$ it is received from (2.11)

$$c = \frac{r_1^2 b}{2\nu} - 1, \quad A_0 = \frac{r_1^3 b^2 v_0 \exp(0,5)}{2\nu^2}. \tag{2.12}$$

Let at initial time moment the vortex be horizontally spread so as $r_1 \gg 2\nu/b$. In this case r decreases with time until reaching the value $r_m = \sqrt{2\nu/b}$ at $t \gg \frac{ln(c)}{b}$. In it's turn v_m increases at the beginning and then decreases to zero. Substituting $t_m = \frac{1}{b}\ln(\frac{c}{2})$ into (2.11) the value of absolute maximum of rotative component $v = v_{max}$ is given as:

$$\text{at} \quad t = t_m \quad \text{and at} \quad r_m = r_2 = \sqrt{\frac{6\nu}{b}}, \quad v = v_{max} = v_0 r_1 \sqrt{\frac{2b}{27\nu}}. \tag{2.13}$$

It is not difficult to calculate in what times increase v_{max} as v_0 at maximum development stage (at $t = t_m$, and $r = r_m$):

$$n = \frac{v_{max}}{v_0} = r_1\sqrt{\frac{2b}{27\nu}} = \frac{2}{3}\frac{r_1}{r_2}. \tag{2.14}$$

Therefore rotative component increases at maximum development stage with increasing of r. It is not difficult to show that $\Gamma = v_m r_m$ reaches it's absolute maximum at initial moment and $\Gamma_m \to 0$ at $t \to \infty$. Therefore simplified model describes the dissipation of rotative moment. Increasing of vortex in analitic and numerical model is a result of redistribution of angular moment due to a convergence. However constriction of vortex to axis is stoped at $a \approx b/(2\nu)$ (that is at $t > \ln(c)/b$). At this time horizontal advection is compensated by turbulent diffusion. Therefore in both numerical and analytic models the stage of vortex dissipation follows the stage of increasing.

2.4. Simplified analytic model for explanation of exchange of convective cell structure at maximum development stage

Assume that exchange of cell structure is due to interaction of nonlinear items and items allowing for pressure gradient. Let us write the thermodynamic equations received by theory of convection and of vertical boundary layer, neglecting nonstationary, turbulent viscosity and influence of Archimed's forses

$$\begin{aligned} u\frac{\partial w}{\partial r} + w\frac{\partial w}{\partial z} &= -R\theta_0 \frac{\partial}{\partial z}\frac{p'}{P}, \\ u\frac{\partial v}{\partial r} + w\frac{\partial v}{\partial z} + \frac{uv}{r} &= 0, \\ v^2 &= R\theta_0 \frac{\partial}{\partial r}\frac{p'}{P}, \\ \frac{\partial ur}{\partial r} + \frac{\partial wr}{\partial z} &= 0 \end{aligned} \tag{2.15}$$

with boundary conditions

$$\text{at} \quad r = 0 \quad u = v = 0 = \frac{\partial w}{\partial r} = \frac{\partial p'}{\partial r} = 0, \tag{2.16}$$

$$\text{at} \quad r = \infty \quad u = v = w = 0, \tag{2.17}$$

$$\text{at} \quad z = \infty \quad u = v = w = 0, \tag{2.18}$$

Let us note that the number of conditions is greater than the order of the system (2.16)–(2.18). But the solution of the problem shall be showed to be possible.

Introduce the current function ψ according to these relationships

$$w = \frac{1}{r}\frac{\partial \psi}{\partial r}, \quad u = -\frac{1}{r}\frac{\partial \psi}{\partial z}. \tag{2.19}$$

Substituting (2.19) into (2.15) it is obtained

$$-\frac{\partial\psi}{\partial z}\frac{\partial^2\psi}{\partial z^2}+\frac{\partial\psi}{\partial y}\frac{\partial^2\psi}{\partial y\partial z}=-R\theta_0\frac{\partial}{\partial z}\frac{p'}{P}, \tag{2.20}$$

$$-\frac{\partial\psi}{\partial z}\frac{\partial\Gamma}{\partial y}+\frac{\partial\psi}{\partial y}\frac{\partial\Gamma}{\partial z}=0, \tag{2.21}$$

$$R\theta_0\frac{\partial}{\partial y}\frac{p'}{P}=\frac{\Gamma^2}{4y^2}\quad\left(\frac{\partial\psi}{\partial y}=w,\quad\frac{\partial\psi}{\partial z}=-\sqrt{2y}u\right). \tag{2.22}$$

The equation (2.21) is the Jacobian and reflects functional connection between Γ and ψ. Assuming this connection to be linear, we have

$$\Gamma=c_0\psi,\quad c_0=const. \tag{2.23}$$

Differentiating (2.20) with respect to r, a (2.22) with respect to z, adding equations and allowing for (2.23) we receive

$$\frac{\partial\psi}{\partial z}\frac{\partial^3\psi}{\partial y^3}+\frac{\partial\psi}{\partial y}\frac{\partial^3\psi}{\partial y^2\partial z}=\frac{c_0^2}{2y^2}\psi\frac{\partial\psi}{\partial z}. \tag{2.24}$$

If the variables can be separated, we have instead of (2.24) the following:

$$\psi=F(z)f(z);\quad F\frac{dF}{dz}\left(ff'''-f'f''-\frac{c_0^2f^2}{2y^2}\right)=0\quad\left(f'=\frac{\partial f}{\partial y}\right). \tag{2.25}$$

Therefore if F is bounded function with bounded derivative, then f satisfies the following equation

$$\frac{ff'''-f'f''}{f^2}=\frac{c_0^2}{2y^2}. \tag{2.26}$$

Integrating (2.26), after simple transformations one receives

$$f''+\frac{c_0^2}{2y}f-c_1f=0;\quad c_1=const. \tag{2.27}$$

The solution (2.27) has the following form

$$f=y\exp(\sqrt{c_1}y)\pi(\alpha_0,\varepsilon y);\quad\alpha=1-\frac{c_0^2}{4\sqrt{c_1}};\quad\varepsilon=2\sqrt{c_1}; \tag{2.28}$$

$$\pi(\alpha_0,\varepsilon y)=1+\frac{\alpha_0(\varepsilon y)}{1!2!}+\frac{\alpha_0(\alpha_0+1)(\varepsilon y)^2}{2!3!}+\frac{\alpha_0(\alpha_0+1)(\alpha_0+2)(\varepsilon y)^3}{3!4!}+\ldots$$

Analysis of (2.28) shows that at $\alpha_0>0$ the conditions (2.17) are not satisfied ; at $\alpha<0$ one is satisfied but f can change the sign. That means

that different parts of vortex can have an opposite sense of rotation what is not possible. The solution at $\alpha = 0$ is deprived of pointed out weakness. It is in the form

$$f = y \exp\left(-\frac{c_0^2}{4} y\right), \quad c_1 = \frac{c_0^4}{16}. \tag{2.29}$$

Let $c_0 = 2\sqrt{2}/r_0$, where r_0 – radius of the central part of vortex (it's core). Substituting (2.29) into the expression for meteofield and returning to coordinate r we receive

$$\begin{aligned} w &= \left(1 - \left(\frac{r}{r_0}\right)^2\right) \exp\left(-\left(\frac{r}{r_0}\right)^2\right) F; \quad v = \sqrt{2}\frac{r}{r_0} \exp\left(-\left(\frac{r}{r_0}\right)^2\right) F; \\ u &= -\frac{r}{2} \exp\left(-\left(\frac{r}{r_0}\right)^2\right) \frac{dF}{dz}; \quad p' = -\frac{P}{2R\theta_0} \exp\left(-2\left(\frac{r}{r_0}\right)^2\right) F^2. \end{aligned} \tag{2.30}$$

Then assume $F(z) > 0$. In this case the air ascends within the vortex core $w > 0$ at $r < r_0$ and one descends at it's periphery $w < 0$ at $r > r_0$. It must be noted, it is vortex core that is the visible part of whirlwind due to the presence of opaque particles lifted from the surface by powerfull stream. It is not difficult to calculate that maximum upward speed is more greater downward one at the same heights. Rotative component of motion reaches the maximum value at the vortex core: $v = v_{max} = \exp(-0,5)F$ at $r = r_0/\sqrt{2}$. v rapidly decreases with increasing r. Vertical structure of the meteofields is defined by the function F. Due to surface is impervious to the air particles, we have $F = 0$ at $z = 0$. Then F rapidly increase up to heights of several meteres ($dF/dz > 0$). Outside of this region $u < 0$ air is moving to the vortex axis. Then, according to the observation, for the space of 1 kilometere and more visible vortex part slightly depends on height. We shall believe $F \approx const$, $u \approx 0$ in this region. It becomes weak ($dF/dz < 0$) for the big height near the cloud giving rise to whirlwind. In this part of vortex $u > 0$ and air particle, moving from the centre, find itself at the whirlwind periphery being region of downward motion. Reaching the surface's part of the vortex, particles find itself again at whirlwind core. Therefore in this model air particles stay in reserved local region, which is little more than some cubic kilometeres. It is realy observed air can be at relative rest near the whirlwind. According to the theory the rotative and vertical speed component are not too different from each other: $w_{max}/v_{max} = \exp(0,5)$. Approximate estimations obtained in [7] by measuring of particles speed show that rotative and vertical components are approximatly equal. Analysis of the solution and comparision with experimental data carried out show that analytic model elaborated gives the results closed to really situation at the stable stage of whirlwind. Under

real conditions duration of that stage is rarely longer than a few minutes. In consequence we note that it is convenient for calculations to use value v_{max} instead of F:

$$v_{max} = F\exp(-0,5). \tag{2.31}$$

Therefore in the proposed model all variables can be exspressed through v and r determined from observation data.

2.5. United analytic model of vortex

Comparing (2.7), (2.9) with (2.30) one sees the closeness of relationships for v in the both cases. Let us determine the conditions, under which these solutions coincide. Let the field of u and w set within the vortex in accordance with (2.1). Introduce the independent on z deviations resulted from the vortex

$$w = bz + w'(r,t), \quad T = \theta(z) + \vartheta'(r,t), \quad u' = 0. \tag{2.32}$$

Equations for deviations are the following

$$\frac{\partial w'}{\partial t} - \frac{br}{2}\frac{\partial w'}{\partial r} = \lambda\vartheta' + \frac{\nu}{r}\frac{\partial}{\partial r}r\frac{\partial w'}{\partial r}, \tag{2.33}$$

$$\frac{\partial \vartheta'}{\partial t} - \frac{br}{2}\frac{\partial \vartheta'}{\partial r} = \alpha w' + \frac{\nu}{r}\frac{\partial}{\partial r}r\frac{\partial \vartheta'}{\partial r}. \tag{2.34}$$

Let $\vartheta' = \sqrt{\alpha/\lambda}w'$ and $y = r^2/2$. Then it is received instead of (2.33)–(2.34)

$$\frac{\partial w'}{\partial t} - by\frac{\partial w'}{\partial y} = \sqrt{\alpha\lambda}w' + 2\nu\frac{\partial}{\partial y}y\frac{\partial w'}{\partial y}. \tag{2.35}$$

Substituting $w' = \frac{\partial\psi}{\partial y}$ into (2.35) and integrating it with respect to y we obtain

$$\frac{\partial \psi}{\partial t} - by\frac{\partial \psi}{\partial y} = (\sqrt{\alpha\lambda} - b)\psi + 2\nu y\frac{\partial^2\psi}{\partial y^2}. \tag{2.36}$$

Introducing new function $\psi = \exp((\sqrt{\alpha\lambda} - b)t)\psi_1$ and substituting it into (2.36) we have

$$\frac{\partial \psi_1}{\partial t} - by\frac{\partial \psi_1}{\partial y} = 2\nu y\frac{\partial^2\psi_1}{\partial y^2}. \tag{2.37}$$

Comparing (2.37) with (2.5) one sees their coincidence. Therefore

$$\psi = \psi_0\exp((\sqrt{\alpha\lambda} - b)t)A(t)y\exp(-ay), \quad \Gamma = Ay\exp(-ay), \tag{2.38}$$

where a and A is gived by (2.9), $\psi_0 - const$.

Comparing (2.38) with the analytic solution of nonlinear model (2.15)–(2.18) we obtain:

$$\Gamma = cFy\exp\left(-\frac{c^2y}{4}\right), \quad \psi = Fy\exp\left(-\frac{c^2}{4}\right). \tag{2.39}$$

It is obvious that (2.38) and (2.39) coincide in the case

$$\Gamma = A, \quad c = 2\sqrt{a}, \quad c = \psi_0\exp((\sqrt{\alpha\lambda} - b)t). \tag{2.40}$$

Note that F and c can depend on time. The unsteady-state of process is allowed for (2.33), (2.34). The last two relationships at (2.40) mean that

$$2\sqrt{\frac{b\exp(bt)}{2\nu(\exp(bt)+c_1)}} \approx \psi_0\exp((\sqrt{\alpha\lambda} - b)t), \quad c_1 = \frac{r_1^2b}{2\nu} - 1 \approx \frac{r_1^2b}{2\nu}. \tag{2.41}$$

Approximate equality (2.41) takes place only at the beginning of process by carrying out the following conditions

$$t \ll \frac{1}{\ln(c_1)}, \quad \sqrt{\alpha\lambda} = \frac{3b}{2}, \quad \psi_0 = \sqrt{\frac{2b}{\nu c_1}} = \frac{2}{r_1} \tag{2.42}$$

and at the stage of it's dissipation also by carrying the conditions

$$t \gg \frac{1}{\ln(c_1)}, \quad \sqrt{\alpha\lambda} = b, \quad \psi_0 = \sqrt{\frac{2b}{\nu}} = \frac{2}{r_1}. \tag{2.43}$$

There is the third condition: the process have to be independent or slightly dependent on z. Therefore the situations are possible when nonlinear items are compensated by pressure gradient, the process becomes quasy-linear, quasy-laminar. In these situations gradient catastrophe becomes unlikely and the convective cell stability is essentially enhansed in spite of formations have vertical scale being considerable more than horisontal one. In that vorteces time changes are conditioned on the whole by advective transfer, resulting in concentration of rotative moment near axis, and turbulence, resulting in the dissipation of rotative moment.

The picture adduced is confirmed by observation data: constriction of rotative vortex occures apparently in mother's cloud giving rise to vortex. Under sufficiently rapid rotation nonlinear items are compensated by pressure gradient, vertical scale rapidly increases until vortex reaches the surface. Increasing of vertical scale is accompanied by increasing of rotation speed of vortex and essentially vertical motion component. And, after all, proposed analytic model explains relative rarity of atmospheric vortexes.

The presence of angular moment in atmosphere is an ordinary situation essentially under cyclonic conditions. However, it is not difficult to calculate that the time of constriction of angular moment towards process's axis is greater than the average time convective cell existing, i.e., vorticies have no time to arise.

2.6. Numerical model of axisymmetric tropical cyclone

Mature tropical cyclone is understood to be a self-supporting thermohydrodynamic mesoscale system. Energy for it's maintainance is drawing in great part from the convective latent heat release. For reason given a reserchers face problem of parameterization or, whenever possible, description with detail the processes connected with phase transition and precipitation in the construction of tropical cyclone model [7]. It is not the purpose of this paper to trace the complete history of research in this area or to summarize all of the current parameterization schemes. We address to cumulus parameterization only as to the possible mean of account of the smallscale convective pulsation giving rise to the gigantic convective cell – tropical cyclone. Let us note that the results obtained in the previous parts of the paper can be used for construction of parameterization relationships too.

Let us write a mathematical model of this phenomenon. Simplifications of the vertical boundary layer theory are inapplicable in this case as opposed to the models of thunderstorm and tornado. We shall use system of the deep convection equations. Consider the axisymmetric hurricane models. The equations are given as follows:

$$
\begin{aligned}
&\frac{\partial u}{\partial t} + u\frac{\partial u}{\partial r} + w\frac{\partial u}{\partial z} - \frac{v^2}{r} = -R\theta\frac{\partial}{\partial r}\frac{p'}{P} + fv + \frac{\partial}{\partial r}\frac{\nu}{r}\frac{\partial ur}{\partial r} + \mu\frac{\partial^2 u}{\partial z^2},\\
&\frac{\partial v}{\partial t} + u\frac{\partial v}{\partial r} + w\frac{\partial v}{\partial z} + \frac{uv}{r} = -fu + \frac{\partial}{\partial r}\frac{\nu}{r}\frac{\partial vr}{\partial r} + \mu\frac{\partial^2 v}{\partial z^2},\\
&\frac{\partial w}{\partial t} + u\frac{\partial w}{\partial r} + w\frac{\partial w}{\partial z} = -R\theta\frac{\partial}{\partial z}\frac{p'}{P} + g(\vartheta/\theta + 0.61q) + \frac{\nu}{r}\frac{\partial}{\partial r}r\frac{\partial w}{\partial r} + \mu\frac{\partial^2 w}{\partial z^2},\\
&\frac{\partial \vartheta}{\partial t} + u\frac{\partial \vartheta}{\partial r} + w\frac{\partial \vartheta}{\partial z} = -w\frac{\partial \theta}{\partial z} + \frac{\nu}{r}\frac{\partial}{\partial r}r\frac{\partial \vartheta}{\partial r} + \mu\frac{\partial^2 \vartheta}{\partial z^2} + F_1, \qquad (2.44)\\
&\frac{\partial q}{\partial t} + u\frac{\partial q}{\partial r} + w\frac{\partial q}{\partial z} = -w\frac{\partial Q}{\partial z} + \frac{\nu}{r}\frac{\partial}{\partial r}r\frac{\partial q}{\partial r} + \mu\frac{\partial^2 q}{\partial z^2} + F_2.
\end{aligned}
$$

The notations used are:

t – time;

r, z – cylindrical radial and vertical coordinates;

u, w, v – radial, vertical and tangential components of velocity correspondingly;

ϑ, q, p' – temperature, moisture and pressure deviation from it's values $\theta(z)$, $Q(z)$, $P(z)$ in undisturbed atmosphere;

$\rho(z)$ – density in undisturbed atmosphere;

R – gas constant of the dry air;

f – the Coriolis parameter;

g – gravitational acceleration;

F_i, $i = 1, 2$ – convective fluxes;

ν, μ – kinematic turbulent coefficients.

It should be remarked that ν and μ vary in a physical sense; the former describes the average vertical distribution of turbulence within the individual convective clouds, and the latter – large-scale horizontal distribution of turbulence, for which convective clouds are the individual pulsations.

Let us address to numerical results. The time integration of hurricane model was carried out. They show that a weak cyclonic disturbance setting in initial moment transforms by cloudy convection to hurricane of middle intensivity. Moist convection was parameterized by several methods – Kuo [14], massflux (bulk-model) [29] and method with detailed mycrophysic [11].

By the early second day the circulation of identical type is formed in all numerical calculations. Air motion in vertical section of atmosphere consists of two cells with various sizes, intensivities and the senses of circulation. Inner small cell provides with relatively powerfull downward currents on the hurricane axis and weaker upward motion at a range $200 - 1000km$ from the axis. The external greater cell has inverse sense of circulation and it is it that provides typical cyclonical distribution of the flow with convergence in the lower part of hurricane and divergence in one's upper part. Region of upward motion of both cells coalesce. Therefore the air particles transfer vaporous and liquid water in wide ring with area of $\sim 10km$, significantly intensifying the procceses of precipitation (if they are accounted for). In it's turn condensation and precipitation magnify intensivity of circulation in the both cells. A region of downward motion concerning to second cell is at the periphery of TC, that is conditioned by Coriolis's forces action. Intensivity of tangential and radial velocity components are closely related, and the sense of rotation is cyclonic in the lower and middle parts of TC. In the upper troposphere the vortex has an inverse sense of rotation.

3. Conclusion

The studies conducted allow the following conclusions:

- the heat of convective turbulence is convective cell;
- convective cell is unstable to a finite-amplitude disturbances;
- stability of cells is determined by external model's parameters and decrease with time;
- complicated nature of convective turbulence is conditioned by interaction between cells resulting in their coagulation or destruction;
- the model accounts for only interaction of cells located over each other. This and a number of simplifications for setting up a problem make possible to construct the convective cells's distribution function depending on their sizes, existence time and large-scale parameters;
- there are three ierarchy levels of convective formations in atmosphere, that are small-scale convective turbulence, thermals and cumulus clouds, convective ensembles;
- rotation of convective cells causes their stability to increase;
- by enhanced stability of rotating cells the relatively weak thermals and cumulus clouds transform to whirlwind or tornado;
- tropical cyclones may be considered to be (with minor reservations) large-scale analog of whirlwind. In spite of essentially various sizes the space structure and mechanism of these phenomena has much in common, in particular, the type of circulation.

Acknowledgements. We are thankfull to proffesor L. Gutman whose idies formed the basis of the models proposed. This work has been supported financially by Soros's fond.

References

[1] A.D. Amirov, A calculation technique of moisture and temperature fields in the problem on cumulus cloud, Izv. AN SSSR, FAO, Vol. 7, 1971, 723–730 (in Russian).

[2] V. Andreev, S. Pantchev, A Dynamics of Atmospheric Thermals, Hidrometeoizdat, Leningrad, 1975 (in Russian).

[3] A. Arakawa, W.A. Schubert, Interaction of a cumulus cloud ensemble with the large-scale environment, P.L.– J.Atm. Sci., Vol. 31, 1974, 674–701.

[4] H.L. Bizova, V.N. Ivanov, E.K. Garger, A Turbulence in Atmospheric Surface Layer, Hidrometeoizdat, Leningrad, 1989 (in Russian).

[5] Cloud and Cloudy Atmosphere. Handbook. (by edit. N.P. Mazin, A.Ck. Ckrgian), Hidrometeoizdat, Leningrad, 1989 (in Russian).

[6] J.W. Deardorff, Three-dimensional numerical study of turbulence in an entraining mixed layer, Bound.-Layer Meteor., 7, 1974, 199–226.

[7] W.M. Frank, The cumulus parameterization problem, Mon. Wea. Rev., Vol. 111, No. 9, 1983, 1859–1871.

[8] M.A. Goldshtik, On a problem of turbulence, Sbornik nautchnich trudov "Ustoitchivost and turbulentnost", SO AN SSSR, Institut teplofiziki, Novosibirsk, 1985 (in Russian).

[9] L.N. Gutman, On laminar thermal convection above a stationary warmth source, Prikladnaya matematika i mechanika, Vol. 13, 1949 (in Russian).

[10] L.N. Gutman, Introduction in Nonlinear Theory of Mesoscale Meteorological Processes, Hidrometeoizdat, Leningrad, 1969 (in Russian).

[11] E.Kessler, On the Distribution and Continuity of Water Substance in Atmospheric Circulations, Meteorological Monographs, Vol. 10, No. 32, 1969.

[12] D.A. Konovalov, On the problem on thermals 's structure, Trudi GGO, 257, 1970, 123–128 (in Russian).

[13] H.L. Kuo, On formation and intensification of tropical cyclones through latent heat release by cumulus convection, J. Atmos. Sci., Vol. 22, 1965, 40–63.

[14] H. L. Kuo, Further studies of the parameterization of the influence of cumulus convection on large-scale flow, J. Atmos. Sci., Vol. 31, 1974, 1232–1240.

[15] F.H. Ludlam, R.S. Scorer, Bubble theory of penetrative convections, Quart. J. Roy. Met. Soc., Vol. 79, No. 339, 1952.

[16] I.P. Mazin, S.M. Shmeter, Clouds, Structure and Formation Physics, Hidrometeoizdat, Leningrad, 1983 (in Russian).

[17] V.M. Malbackov, An investigation of tornado structure, Izv. AN SSSR, FAO, 1972, 17–28 (in Russian).

[18] V.M. Malbackov, On a theory of thermals in stationary atmosphere, Izv. AN SSSR, FAO, Vol. 8, 1972, 683–694 (in Russian).

[19] V.M. Malbackov, On interaction of thermals, Trudi ZSRNIGMI, 416, 1978, 75–85 (in Russian).

[20] V.M. Malbackow, A simplified model of the convective cells ensemble and a construction of parametrization procedures for moist convection, Izv. AN SSSR, FAO, Vol. 28, 1992, 901–914 (in Russian).

[21] V.M. Malbackov, L.N. Gutman, On a theory of atmospheric vorticies with the vertical axis, Izv. AN SSSR, FAO, No. 6, 1968 (in Russian).

[22] V.M. Malbackov, C.F. Gimelshein, An analytic model of forming of time and space of convective formations in atmosphere, Trudi ZapSibNIGMI, 89, 1989, 18–27 (in Russian).

[23] B.J. Mason, The Physics of Clouds, (second edition), Oxford, 1971.

[24] R. Skorer, Aerodynamics of Environment, Mir, Moscow, 1980 (in Russian).

[25] L.A. Vaskevitch, P.Y. Pushistov, Comparative analysis of a some statistical characteristics of vertical velocity and temperature devitions fields within thermals by numerical modeling and observational data, Trudi ZapSibNIGMI, 85, 1988, 84-91 (in Russian).

[26] L.A. Vaskevitch, P.Y. Pushistov, An occurence frequency and horizontal sizes of thermals in numerical simulations of penetrative convection ensemble in atmospheric surface layer, Trudi ZapSibNIGMI, 85, 1988, 91–97 (in Russian).

[27] J.M. Wilczak, J.A. Businger, Termally indirect motions in the convective atmospheric boundary layer, J. Atmos. Sci., 40, 1983, 343–358.

[28] E.N. Wilkins, Y. Sasaki, E.W. Marion, Laboratory simulation of wake effects on second and third thermals, Mon. Wea. Rev., Vol. 100, 1972, 399–407.

[29] M. Yanai, S. Esbensen, J.H. Chu, Determination of bulk properties of tropical cloud clusters from large-scale heat and moisture budgets, J. Atmos. Sci., Vol. 30, 1973, 611–627.